Construction and Building Materials 169 (2018) 28–33

Contents lists available at ScienceDirect

Construction and Building Materials

journal homepage: www.elsevier.com/locate/conbuildmat

Laboratory investigation of the durability of a new smart geosynthetic material

Jun Li [a], Xin-zhuang Cui [b,*], Qing Jin [a], Jun-wei Su [a], She-qiang Cui [a], Yi-lin Wang [a]

[a] School of Civil Engineering, Shandong University, Jinan 250061, PR China
[b] Shenzhen Institute, Shandong University, Shenzhen 518057, PR China

HIGHLIGHTS

- A new smart geosynthetic named sensor-enabled geobelt (SEGB) was developed.
- The effects of three degradation tests on the durability of SEGB were investigated.
- Mechanical properties and tensoresistivity of SEGB after degradation were evaluated.
- The degradation mechanism of SEGB was analyzed.

ARTICLE INFO

Article history:
Received 4 December 2017
Received in revised form 22 February 2018
Accepted 24 February 2018

Keywords:
Smart geosynthetic
Mechanical properties
Tensoresistivity
Durability

ABSTRACT

The durability of geosynthetics is important for their service life, transportation and long-term storage. This paper presents the effects of three accelerating degradation tests (thermal oxidation, UV radiation and corrosion) on the mechanical properties and tensoresistivity of a new smart geosynthetic material called sensor-enabled geobelt (SEGB), which is made by high-density polyethylene (HDPE) filled with carbon black (CB). Three characteristics obtained by two tensile tests with different loading speeds are considered to evaluate the durability of the SEGB: tensile strength, elongation at break and electrical resistance. The results show that the tensile strength and elongation at break decrease to different degrees. It indicates that the mechanical properties of the SEGB deteriorate after the three degradation tests. And the electrical resistance displays a sharp increase trend after the strain exceeds a certain number. That means the sensitivity of tensoresistivity improves. Furthermore, the degradation mechanism of the SEGB in the three degradation tests is demonstrated. And it indicates that the chain reactions trigger the change of these mechanical properties and the tensoresistivity of the SEGB.

1. Introduction

Geosynthetics is the generic term for a series of sheets or fibroid materials that are primarily applied in geotechnical and environmental engineering [1,2]. And the geosynthetics can appear in multiple forms such as geogrids, geotextiles, geomembranes, geomeshes, geosynthetic clay liners, geomats and geonets. Basically, all of these geosynthetics are made of polymers. After decades of material science development, the polymer used in geosynthetics production has been converted from the original polyamide (PA) to various types such as polypropylene (PP), polyethylene (PE) and polyethylene terephthalate (PET) [3]. Benefiting from the advantages of these polymer materials, most geosynthetics are stable, strong, light, widely available, easy to transport and cost-competitive against other alternatives. Therefore, the emergence and prosperity of geosynthetics in civil engineering are nothing short of remarkable.

Most often, geosynthetics are extensively used in civil engineering projects for reinforcement applications. Examples include the stabilization of highway slopes and embankments [4,5], reinforcement of foundations [6–8], and reinforcement of paved roads to mitigate cracking and rutting [9]. As geosynthetic-reinforced structures become more globally widespread, it becomes increasingly vital to ensure that these structures are safe and offer a satisfactory level of serviceability through health monitoring and timely measures to prevent catastrophic failures. One of the most important aspects of health monitoring in geosynthetic structures is to monitor the geosynthetic strain during the service life and extreme (e.g., seismic) events. Therefore, many attempts to measure soil strains and in-soil reinforcement strains include the use of digital imagery, X-rays, tomographic techniques and fiber optic cable

* Corresponding author.
E-mail address: cuixz@sdu.edu.cn (X.-z. Cui).

https://doi.org/10.1016/j.conbuildmat.2018.02.187
0950-0618/

[10–16]. However, the limited monitoring scope of these techniques renders them impractical for field-scale structures. Consequently, smart geosynthetic materials that are made from conductive polymer composites are attempted for use in monitoring areas. Existing research shows that using carbon black as filler can make the polymer composite conductive [17–19], and its conductivity certainly changes with pressure, tension, temperature, etc. Therefore, the smart geosynthetics made from this type of material have great potential in the monitoring of numerous fields of engineering [20].

Hatami et al. proposed a new concept called the sensor-enabled geogrid (SEGG) to add a self-sensing function to conventional geosynthetics by adding a critical concentration of CB to the polymers [21]. This function affords geosynthetics a unique and significant characteristic, by which their tensile strain can be more conveniently measured than the conventional monitoring methods. However, an important unsolved problem remains in the referenced SEGG studies: the strain-conductivity response of SEGG materials with multiple ribs is complex, and the accuracy of the measurement results cannot be fully ensured [22]. Therefore, to ensure the measurement accuracy, a new smart geosynthetic named sensor-enabled geobelt (SEGB) was developed by the authors [23]. The SEGB of high-density polyethylene (HDPE) filled with carbon black (CB) was fabricated in both industry and laboratory. A series of in-isolation tests or in-soil tests was performed to study its mechanical properties and tensoresistivity performance.

In addition to being used as reinforcements, SEGBs are also used in other fields such as landfills, deep foundations, and waste disposal. The environment of these engineering applications is extremely complex and often accompanied by high temperature, high heat, radiation, and acidic/alkaline liquids. These aspects have raised the requirements for the durability of SEGBs. In addition, SEGBs are expected to have favorable durability during the service life, transportation and long-term storage. However, durability studies of SEGB or SEGG remain scarce. In contrast, the studies on the durability of polymer materials have more results. For example, several long-term durability tests of polyolefin geotextiles were compared with the oxidative resistance of HDPE by Mueller [24]. The results show that the lifetime of the HDPE is essentially determined by the slow loss of stabilizers, and the mechanical property degradation strongly depended on the oxidation conditions. Lodi found that only the ultraviolet part of light was harmful to the geosynthetic materials, and each material was sensitive to a particular wavelength [25]. The main reactions in the degradation of HDPE during long-term aging were presented by Kriston and Mitroka [26,27]. Zanasi demonstrated a series of suitable accelerated aging methods of HDPE [28]. These studies add great value to the durability study of SEGB from content to method.

Therefore, to evaluate the durability performance of SEGB, three experiments were performed to explore the effects of adverse conditions (thermal oxidation, ultraviolet radiation and acid/alkaline corrosion) on the mechanical properties and tensoresistivity of the SEGB.

2. Fabrication and features of SEGBs

2.1. Materials and production processes of SEGBs

Two types of raw materials were used to make SEGBs: virgin polymer using a high-density polyethylene (HDPE) and a conductive masterbatch using super conductive carbon black (masterbatch of CB). Because the components of the super conductive carbon black and their contents were disclosed by the supplying companies, the filler content of the CB-filled SEGB specimen in this paper was the mixing ratio of the conductive masterbatch to the virgin polymer (HDPE) instead of the actual content. Table 1 shows three parameters of the HDPE.

First, the masterbatch of CB was manually mixed with HDPE until the polymer beads appeared to be evenly distributed in the mix. Then, the mixture was extruded using a twin-screw extruder with a mixing section. All polymer pellets in the batch should be preheated and completely and uniformly melted. The temperatures in the working zones of the extruder were set to 180 °C, 185 °C, 190 °C, 200 °C, 213 °C, and 205 °C. The compounding procedure began after reaching the target temperature, and the mixture was melted in the working zones. The compounding procedures began after reaching the target temperatures, and the pellets melted in the working zones. Once extruded, the samples were compression-molded.

2.2. Determination of the percolation region

As the filler, the content of carbon black significantly affects the conductivity of the SEGB. Therefore, the optimal mixing ratio of black carbon and HDPE is important to find before the production of SEGBs. This optimal mixing ratio can be derived from the percolation theory [19,21], and the percolation phenomenon is shown in Fig. 1. Specifically, first, a batch of samples with different carbon black contents should be made. Then, a variation curve of the surface resistivity with the CB content can be certain based on a test. Finally, the carbon black content at the sharp turning point of resistance is the optimal value. The test is as follows:

The CB and HDPE mixture was poured into a prepared steel mold and pressed for 10 min at 180 °C. Then, the mold is put into the laboratory plate vulcanizing press machine to cool under a 24 MPa compressive stress [19,21]. The specimen with the dimensions of 160 mm × 110 mm × 4 mm is obtained.

The specimen and stick conductive tapes are cleaned on the measuring points, and the surface resistance can be measured with a FLUKE insulation tester. The surface resistivity is defined as follows:

$$\rho_s = R_s \frac{l}{d} \tag{1}$$

where ρ_s is the surface resistivity; R_s is the surface resistance; d is the electrode distance perpendicular to the two conductive adhesive tapes; l is the electrode length.

Fig. 2 shows the variation curve of the surface resistivity with the CB content. At the point of 47.5%, the surface resistivity has a sharp decrease. Hence, the optimum CB content value was 47.5%. The SEGBs in this paper were produced based on this CB content.

2.3. Mechanical properties of SEGBs

The tensile strength and elongation at break are two extremely important mechanical indices. Specifically, the elongation at break refers to the ratio of the sample length after breakage to its original length. Both tensile strength and elongation at break can be obtained through tensile test I.

Tensile test I was strictly performed according to the Plastics-Determination of tensile properties [29]. Fig. 3 shows the dimensions (160 mm × 15 mm × 1.7 mm) of the SEGB specimen in tensile test I. Tensile test I was performed on a universal testing

Table 1
Physical properties of HDPE.

Density (kg/m^3)	Tensile strength (MPa)	Elongation at break (%)
0.954	26	500

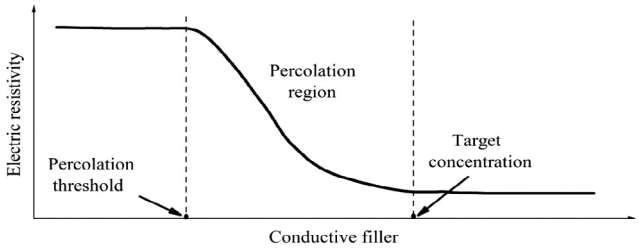

Fig. 1. Percolation phenomenon in conductive polymer composites.

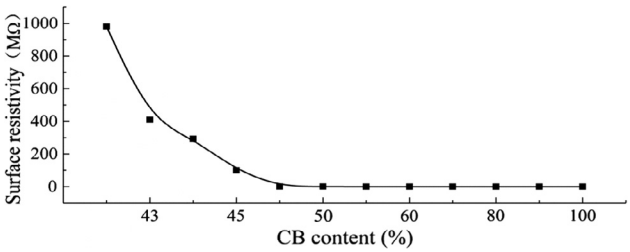

Fig. 2. Variation curve of the surface resistivity of the CB/HDPE specimen.

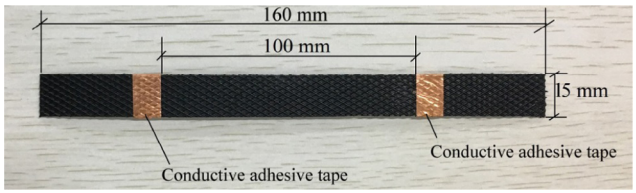

Fig. 3. SEGB specimen for tensile tests.

machine at the tensile loading speed of 20 mm/min, until the specimen broke. The tensile strength was recorded at all times in the experiment. To avoid accidental errors, three SEGB samples were used as a set in each run, and the data were averaged. Fig. 4 shows a typical variation curve of the stress with strain of the SEGB.

2.4. Tensoresistivity of SEGBs

Tensoresistivity is a professional term to define the strain sensitivity of the conductivity of SEGBs. More specifically, it indicates that the surface resistance changes with different strains of SEGBs. To analyze the change in tensoresistivity, the surface resistance was measured by tensile test II and normalized as follows:

$$k = \frac{R_s}{R_{so}} \tag{2}$$

where k is the normalized resistance; R_{so} is the original resistance; R_s is the resistance with strain.

As shown in Fig. 3, the dimensions (160 mm × 15 mm × 1.7 mm) of the specimen in tensile test II were identical to that in tensile test I. Tensile test II was also performed on the universal testing machine. However, the loading speed was cycled at 0.25 mm/min in the first minute. Then, the loading speed became 0.001 mm/min and was maintained for 3 min until the strain reached 16%. Thus, the mode can simulate the actual situation to the maximum extent through a slow loading while shortening the period as much as possible. The surface resistance R_s was recorded at the end of each cycle. Fig. 5 shows a typical variation curve of the normalized resistance of the SEGB.

3. Durability test of SEGBs

As previously mentioned, SEGBs can be used in some extreme environments. During the transportation, long-term storage or service life, the durability performance of SEGBs may be affected by many adverse conditions. Therefore, three typical accelerating-aging experiments (thermal oxidation, ultraviolet radiation and acid/alkaline corrosion) were performed to investigate the effects of high heat, ultraviolet and corrosive liquid on the mechanical properties and tensoresistivity of SEGB.

The dimensions (160 mm × 15 mm × 1.7 mm) of the specimen in these three tests are identical as shown in Fig. 3.

3.1. Thermal oxidation test of SEGBs

The purpose of the thermal oxidation test was to investigate the effects of high heat on the SEGB. In the laboratory, a DHG-202 oven was used to accelerate the aging process. First, all SEGB specimens in the test were cleaned. Then, the specimens were placed into the DHG-202 oven. The temperature in the test was 100 °C, and the oxygen ratio was 21% [30,31]. The entire experiment lasted 28 days, and every 7 days, a batch of specimens was taken out for tensile tests to evaluate the change in mechanical properties and tensoresistivity.

3.2. Ultraviolet radiation test of SEGBs

The purpose of the ultraviolet radiation test was to investigate the effect of ultraviolet exposure on the SEGB. The LX-2130 ultraviolet aging oven was used to accelerate the aging process. The test temperature was controlled at 20 ± 2 °C. Meanwhile, the humidity was set at 30%. During the test, the SEGB specimens were exposed to the ultraviolet radiation for 20 h every day. Then, 4 h apart, another round of exposure began [32]. Every 7 days, a batch of specimens was taken out for tensile tests to evaluate the change in mechanical properties and tensoresistivity. The entire test process lasted 35 days.

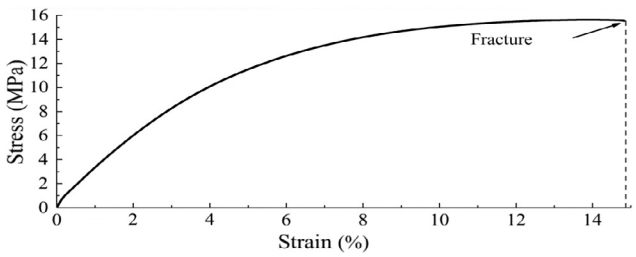

Fig. 4. Variation curve of the stress with strain of SEGB.

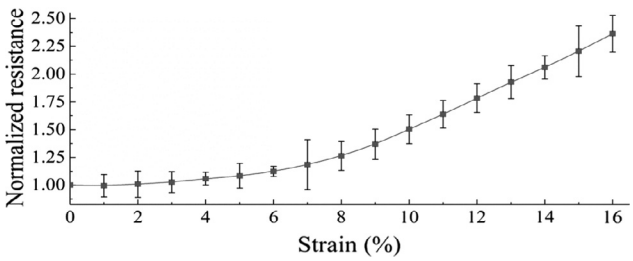

Fig. 5. Variation curve of the normalized resistance of the SEGB.

3.3. Corrosion test of SEGBs

The purpose of the corrosion test was to investigate the effect of acid and alkaline on the SEGB specimens. Two types of solutions were used in this experiment: 0.25 mol/L H_2SO_4 and 0.25 mol/L NaOH [33]. All specimens were separately immersed in two solutions for 60 days. Then, on the 14th, 30th and 60th days, some specimens were taken out for tensile tests to evaluate the change in mechanical properties and tensoresistivity. The temperature was set at 20 °C throughout the experiment. The pH had to be measured every 3 days so that the solute could be replenished in time to maintain its original concentration.

4. Results and discussion

4.1. Mechanical properties of SEGBs

To clearly reflect the change in tensile strength before and after the three tests, a ratio of tensile strength is used and is defined in Eq. (3):

$$R_t = \frac{\sigma_u}{\sigma_{uo}} \tag{3}$$

where R_t is the ratio of tensile strength; $\sigma_{uo}$is the tensile strength before the tests; σ_u is the tensile strength measured during the tests.

Analogously, a ratio of elongation at break is defined in Eq. (4):

$$R_e = \frac{E_u}{E_{uo}} \tag{4}$$

where $R_e$is the ratio of elongation at break; $E_{uo}$is the elongation at break before tests; E_u is the elongation at break measured during the tests.

4.1.1. Tensile strength and elongation in the thermal oxidation test

Fig. 6 shows the variation in R_t and R_e of the SEGB caused by thermal oxidation aging. As displayed in Fig. 6, compared with the initial specimen, the tensile strength and elongation at break after aging demonstrate a distinct decreasing trend. Moreover, for the elongation at break, the reduction rate is accelerating. Meanwhile the variation amplitude of the tensile strength is also slighter than that of the elongation at break.

4.1.2. Tensile strength and elongation in the ultraviolet radiation test

Fig. 7 shows the variation of R_t and R_e of the SEGB caused by ultraviolet radiation aging. Obviously, for the reduction rate or variation amplitude, the trends of the tensile strength and elongation at break are exceedingly similar. Moreover, the reduction amplitude of the tensile strength and elongation at break is small. In fact, both ratios finally decrease to approximately 0.95 after the test. It is due to the CB. The SEGB contains a large amount (47.5%) of CB, which is widely used as an ultraviolet stabilizer in polymers [34]. Specifically, carbon black absorbs ultraviolet radiation and dissipates the absorbed-energy as heat. Thus, the chemical reactions of the degradation process (described in Section 4.3) are retarded because of the lack of energy [34].

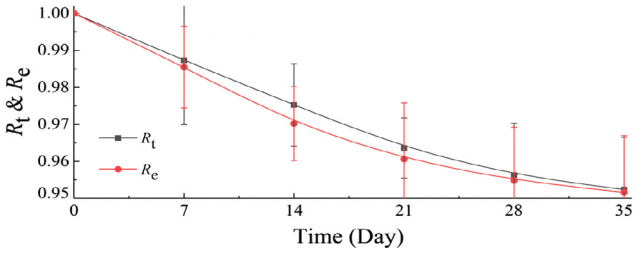

Fig. 7. Variation curves of R_t and R_e in ultraviolet radiation test.

4.1.3. Tensile strength and elongation in the corrosion test

Fig. 8 shows the variation of R_t and R_e of the SEGB caused by acid and alkali corrosion, respectively. As noticed, the tensile strength of the SEGB after the acid corrosion is slightly lower than that after the alkali corrosion. However, the elongation at break after the acid corrosion is slightly higher than that after the alkali corrosion. More specifically, the ratio of tensile strength after the acid and alkali corrosion is approximately 0.87 and 0.89, respectively. The ratio of elongation at break after the acid and alkali corrosion is approximately 0.82 and 0.79, respectively.

4.2. Tensoresistivity of SEGBs

Figs. 9–11 show the variation of the normalized resistance with strain of the SEGB during the thermal oxidation, ultraviolet radiation and corrosion tests, respectively. The results of these experiments show remarkably consistent variation trends. More specifically, within 4% of the strain, the normalized resistance remains stable or presents a tiny growth trend. After the strain exceeds 4%, the normalized resistance demonstrates a sharp linear increase. These trends indicate that, after aging or corrosion, the tensoresistivity of SEGB is more sensitive than before. When strain reaches 16%, the normalized resistance is 7 in the ultraviolet radiation, 5.5 in the acid corrosion test and 7 in the alkali corrosion test, but in the thermal oxidation test, the normalized resistance is approximately 2.5. Compared to other adverse factors, it indicates that thermal oxidation has less effect on the tensoresistivity of SEGBs.

4.3. Analyses of the degradation mechanism

Actually, the degradation mechanism of the SEGB is related to the free radicals. Free radicals are atoms or groups that have electrons. When its covalent bond breaks, two electrons that form a covalent bond are shared by two fragments to become free radicals. This is called homolysis. And the free radicals are unstable, because the electrons in free radicals are not in pairs. It means that

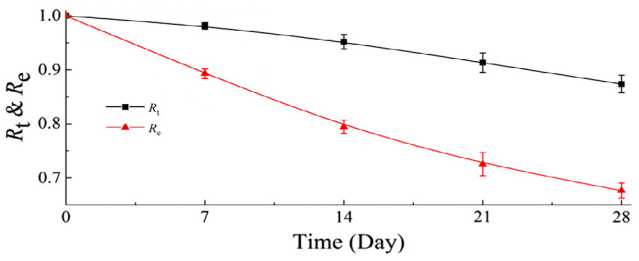

Fig. 6. Variation curves of R_t and R_e in thermal oxidation test.

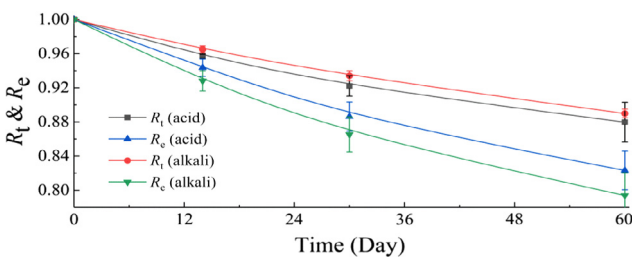

Fig. 8. Variation curves of R_t and R_e in Corrosion Test.

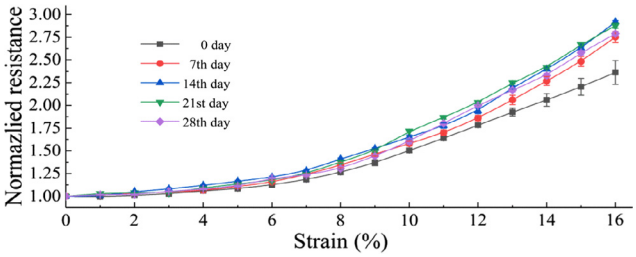

Fig. 9. Variation curve of the normalized resistance with strain in the thermal oxidation test.

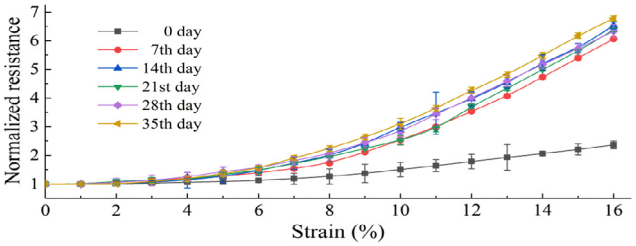

Fig. 10. Variation curve of the normalized resistance with strain in the ultraviolet radiation test.

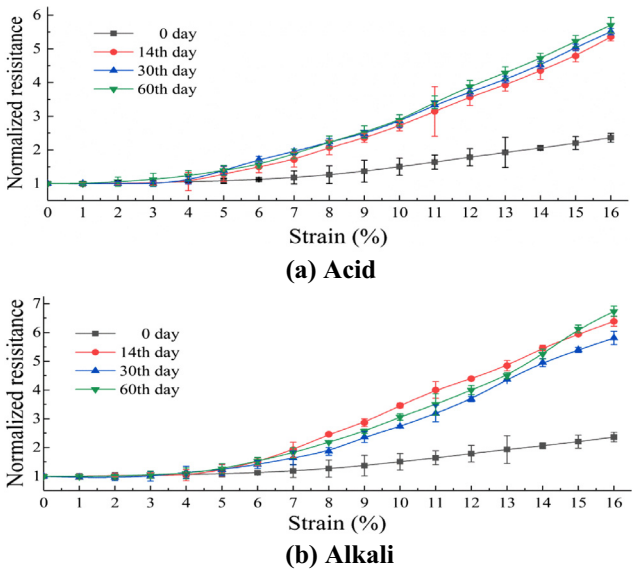

Fig. 11. Variation curve of the normalized resistance with strain in the corrosion test.

free radicals can easily react with other molecules, ions or other free radicals. And these chemical reactions are called chain reactions, as shown in Eqs. (5-1)–(5-14). And there are a lot of recombination covalent bonds in the polymers, because they are synthesized by the process of the polymerization of monomers. Therefore, when the energy is provided, these covalent bonds tend to trigger the hemolysis reaction, producing free radicals. Then, the free radicals do the chain reactions with some molecules, ions or other free radicals. As the process intensifies, the structure of the polymer is destroyed. Therefore, the mechanical performance of the polymer is degraded.

In all durability tests, the thermal oxidation, ultraviolet radiation or corrosion of the chemical liquids with different pH provided the original energy to trigger the chemical reactions. Then, the HDPE in the SEGB was degraded, and the tensile strength or elongation at break decreased to different degrees. Therefore, the thermal oxidation, ultraviolet radiation and chemical liquids play a critical role in the aging or corrosion process of SEGB.

More specifically, the chain reaction has four basic steps: chain initiation, chain propagation, chain branching, chain termination [34]. This is a sequential process, and a series of representative reactions are presented as follows:

$$RH \overset{energy}{\rightarrow} R\cdot + H\cdot \tag{5-1}$$

$$RH + O_2 \overset{energy}{\rightarrow} R\cdot + HO_2\cdot \tag{5-2}$$

$$RH + O_2 + Residual\ catalyzers \overset{energy}{\rightarrow} Free\ Radicals \tag{5-3}$$

Eqs. (5-1)–(5-3) show the initiation reactions energized by temperature or radiation. *RH* is a functional group *R* with a hydrogen *H*. *R*· is a living free radical and the symbol "**·**" means the carried electron. Analogously, the symbol *H*· and HO_2· are all free radicals with the electron.

Because oxygen is present in the environment and many impurities can act as catalysts, the initiation reactions involves these three reactions. In fact, the degradation mechanism is governed by the transport processes of oxygen and other components in the chemical processes. Moreover, there is also an oxidation cycle in the initiation reaction at this stage. And the oxidation cycle is shown in Eqs. (5-4) and (5-5):

$$R\cdot + O_2 \rightarrow RO_2\cdot \tag{5-4}$$

$$RO_2 + RH \rightarrow ROOH + R\cdot \tag{5-5}$$

Then, as shown in Eqs. (5-6)–(5-10), the chain reaction goes on and the free radicals produce by the initiation reaction and the oxidation cycle take part in this process. And at this step, the chain branching reactions and the auto-propagation reactions occurred at the same time. This stage begins when a critical concentration of both *ROOH* and RO_2· reached.

Chain branching reactions are triggered as expressed in Eqs. (5-6)–(5-10):

$$ROOH \rightarrow RO_2 + HO_2\cdot \tag{5-6}$$

$$ROOH + RH \rightarrow RO_2\cdot + R\cdot + H_2O \tag{5-7}$$

$$2ROOH \rightarrow RO\cdot + RO_2\cdot + H_2O \tag{5-8}$$

$$RO\cdot + RH \rightarrow ROH + R\cdot \tag{5-9}$$

$$HO\cdot + RH \rightarrow H_2O + R\cdot \tag{5-10}$$

At last, according to the oxygen condition, the termination reactions among free radicals are divided into two types as shown in Eqs. (5-11)–(5-14), respectively.

Sufficient oxygen supply:

$$2RO_2\cdot \rightarrow RO + ROH + O_2 \tag{5-11}$$

Lack of oxygen:

$$R\cdot + ROO\cdot \rightarrow ROOR \tag{5-12}$$

$$R\cdot + R\cdot \rightarrow RR \tag{5-13}$$

$$R\cdot + RO\cdot \rightarrow ROR \tag{5-14}$$

After this series of reactions, the structure of the HDPE in SEGB will suffer certain damage in different degrees. Therefore, the tensile strength and the elongation at break of the SEGB decrease to different degrees. Moreover, these structure damage leads to the change of the tensoresistivity of SEGB.

More specifically, the conductivity of the SEGB mainly comes from three aspects: the CB fillers are intrinsically conductive. In some parts, CB fillers are directly contacted. And the electron tunneling between the close proximity CB fillers has conductivity. When the structure of the HDPE in SEGB changed, it can trigger the distribution and the local content change of CB. It means that the structure damage of the SEGB finally leads to the change of the CB conductive networks and its electrical resistance. Therefore, the tensoresistivity of SEGB finally changes along with the degradation process.

5. Conclusions

In this paper, the effects of the thermal oxidation, ultraviolet radiation and acid and alkali corrosion on the mechanical properties and tensoresistivity of SEGBs were investigated. The main conclusions are as follows:

(1) After the thermal oxidation aging, because of the degradation, embrittlement and hardening occur in the SEGB, which exhibits different degrees of decrease in tensile strength and elongation at break. The reduction is correlated with the aging time. However, the thermal oxidation aging hardly affects the tensoresistivity.
(2) After the ultraviolet radiation, the tensoresistivity of the SEGB significantly changed. However, the tensile strength and elongation at break hardly decrease. Moreover, the reductions of them are positively correlated with the aging time. In contrast, the tensoresistivity has more correlations with the strain.
(3) After the acid or alkali corrosion, the amplitude of the decrease in tensile strength or elongation at break increases with the aging time, but the rate of decline decreases. The normalized resistance significantly increases and exhibits a high sensitivity of tensoresistivity.
(4) The chain reactions are the internal cause of these mechanical properties and tensoresistivity of the SEGB.

Acknowledgments

This work is supported by the Fund of the Science, Technology and Innovation Commission of Shenzhen Municipality (JCYJ20160429183630760), and the Natural Science Foundations of China (Nos. 51778346, 51479105).

References

[1] B.V. Wiewel, M. Lamoree, Geotextile composition, application and ecotoxicology – a review, J. Hazard. Mater. 317 (2016) 640–655.
[2] T.S. Ingold, Chapter one – Introduction, in: Geotextiles and Geomembranes Handbook, Elsevier, Oxford, 1994, pp. 1–70.
[3] R.M. Koerner, Chapter one – Overview of geosynthetics, in: Designing with Geosynthetics, Pearson Prentice Hall, Upper Saddle River, NJ, 2005, pp. 1–78.
[4] J.N. Mandal, K.S. Jambale, Analysis of a geosynthetic reinforced soil wall by the limit equilibrium method, Constr. Build. Mater. 6 (1992) 173–177.
[5] G.R. Carter, J.H. Dixon, Oriented polymer grid reinforcement, Constr. Build. Mater. 9 (1995) 389–401.
[6] A. Hegde, Geocell reinforced foundation beds-past findings, present trends and future prospects: a state-of-the-art review, Constr. Build. Mater. 154 (2017) 658–674.
[7] L. Zhang, M. Zhao, C. Shi, H. Zhao, Bearing capacity of geocell reinforcement in embankment engineering, Geotext. Geomembr. 28 (2010) 475–482.
[8] J.W. Cowland, S.C.K. Wong, Performance of a road embankment on soft clay supported on a geocell mattress foundation, Geotext. Geomembr. 12 (1993) 687–705.
[9] H.I. Ling, Z. Liu, Performance of geosynthetic-reinforced asphalt pavements, J. Geotech. Geoenviron. Eng. 127 (2001) 177–184.
[10] J. Desrues, R. Chambon, M. Mokni, F. Mzerolle, Void ratio evolution inside shear bands in triaxial sand specimens studied by computed tomography, Geotechnique 46 (3) (1996) 529–546.
[11] R. Luna, Digital image analysis techniques for fiber and soil mixtures, LTRC Project No. 98-2TIRE, Rep. Submitted to the Louisiana Transportation Research Center, Dept. of Civil and Environmental Engineering, Tulane Univ., New Orleans, 1999.
[12] A. Rechenmacher, Imaging-based experimental soil mechanics, in: J.A. Yamamuro, J. Koseki (Eds.), Geomechanics, Testing, Modeling, and Simulation, Proc., 1st Japan-U.S. Workshop on Testing, Modeling, and Simulation, Geotechnical Special Publication No. 143, ASCE, New York, 2003, pp. 653–663.
[13] J. Hironaka, T. Hirai, J. Otani, M. Inoue, Effect of fines concentration in soils on pullout mechanism of geogrid, in: Proc. in GeoAsia 2004, Seoul, Korea, 2004, pp. 357–362.
[14] A.H. Aydilek, M. Guler, T.B. Edil, Use of image analysis in determination of strain distribution during geosynthetic tensile testing, J. Comput. Civ. Eng. 18 (1) (2004) 65–74.
[15] K.A. Warren, I.L. Howard, J.A. Brooks, Use of digital photography to analyze foil strain gages on geosynthetics, in: Geo-Congress 2006: Geotechnical Engineering in the Information Technology Age, ASCE, Atlanta, Georgia, VA, 187(282), 2006, pp. 1–6.
[16] A. Nancey, B. Lacina, J. Henderson, Geotextile and optic fibers: feedback AFTER four years of use in soil, in: Geosynthetics 2007: Proc. GRI-20, Washington, D. C., IFAI, Roseville, MN, 2007.
[17] F. Lux, Models proposed to explain the electrical conductivity of mixtures made of conductive and insulating materials, J. Mater. Sci. 28 (1993) 285–301.
[18] R. Strumpler, J.G. Reichenbach, Feature article conducting polymer composites, J. Electroceram. 3 (1999) 329–346.
[19] J.C. Huang, Carbon black filled conducting polymers and polymer blends, Adv. Polym. Tech. 21 (2002) 299–313.
[20] H. Yazdani, K. Hatami, B.P. Grady, Sensor-enabled geogrids for performance monitoring of reinforced soil structures, J. Test. Eval. 44 (1) (2015), https://doi.org/10.1520/JTE20140501.
[21] K. Hatami, B.P. Grady, M.C. Ulmer, Sensor-enabled geosynthetics: use of conducting carbon networks as geosynthetic sensors, J. Geotech. Geoenviron. Eng. 135 (7) (2009) 863–874.
[22] Q. Chen, Discussion of "Sensor-enabled geosynthetics: use of conducting carbon networks as geosynthetic sensors" by Kianoosh Hatami, Brian P. Grady, and Matthew C. Ulmer, J. Geotech. Geoenviron. Eng. 137 (4) (2011) 435–436.
[23] X.Z. Cui, S.Q. Cui, Q. Jin, Y.L. Wang, L. Zhang, Z.X. Wang, Laboratory tests on the engineering properties of sensor-enabled geobelts (SEGB), Geotext. Geomembr. 46 (2018) 66–76.
[24] W. Mueller, B. Buettgenbach, I. Jakob, H. Mann, Comparison of the oxidative resistance of various polyolefin geotextiles, Geotext. Geomembr. 21 (2003) 289–315.
[25] P.C. Lodi, B.S. Bueno, O.M. Vilar, UV exposure of polymeric geomembranes, in: G.X. Li, Y.M. Chen, X.W. Tang (Eds.), Geosynthetics in Civil and Environmental Engineering, Springer-Verlag, Berlin Heidelberg, 2009, pp. 44–48.
[26] I. Kriston, E. Foldes, P. Staniek, B. Pukanszky, Dominating reactions in the degradation of HDPE during long term ageing in water, Polym. Degrad. Stabil. 93 (2008) 1715–1722.
[27] S.M. Mitroka, T.D. Smiley, J.M. Tanko, A.M. Dietrich, Reaction mechanism for oxidation and degradation of high density polyethylene in chlorinated water, Polym. Degrad. Stabil. 98 (2013) 1369–1377.
[28] T. Zanasi, E. Fabbri, F. Pilati, Qualification of pipe-grade HDPEs: Part I. Development of a suitable accelerated ageing method, Polym. Test. 28 (2009) 96–102.
[29] AQSIQ (General Administration of Quality Supervision, Inspection and Quarantine of the People's Republic of China) & SAC (Standardization Administration of the People's Republic of China), GB/T 1040.1-2006: Plastics – Determination of tensile properties, Standards Press of China, Beijing, 2006.
[30] AQSIQ (General Administration of Quality Supervision, Inspection and Quarantine of the People's Republic of China) & SAC (Standardization Administration of the People's Republic of China), GB/T 17631-1998: Geotextiles and Geotextile-related Products – Test Method for Determining the Resistance to Oxidation, Standards Press of China, Beijing, 1998.
[31] AQSIQ (General Administration of Quality Supervision, Inspection and Quarantine of the People's Republic of China) & SAC (Standardization Administration of the People's Republic of China), GB/T7141-1992: Plastics Methods of Exposure to Thermal Air, Standards Press of China, Beijing, 1992.
[32] AQSIQ (General Administration of Quality Supervision, Inspection and Quarantine of the People's Republic of China) & SAC (Standardization Administration of the People's Republic of China), GB/T 16422.3-1997: Plastics – Methods of Exposure to Laboratory Light Sources – Part 3: Fluorescent UV Lamps, Beijing, 1997.
[33] Z.N. Zheng, Experimental research on the durability of geosynthetics (Dissertation of the degree of Master of philosophy), Chongqing Jiaotong University, 2003.
[34] Y.G. Hsuan, H.F. Schroeder, K. Rowe, W. Muller, J. Greenwood, D. Cazzuffi, Long-term performance and lifetime prediction of geosynthetics, in: 4th European Geosynthetics Conference, 2008.